New Journal of Chemistry

Electronic Supplementary Information for

Chromatographically separable ruffled non-planar isomeric Octaalkylporphycenes: Consequences of unsymmetrical substitution upon structure and photophysical properties

Narendra N. Pati,[a] Sameeta Sahoo,[a] Sipra S. Sahoo,[a] Dipanjan Banerjee,[b]

S. Venugopal Rao[b] and Pradeepta K. Panda*[a]

[a]*School of Chemistry, University of Hyderabad, Hyderabad-500046, India.*

[b]*Advanced Centre of Research in High Energy Materials (ACRHEM), University of Hyderabad, Hyderabad-50006, India.*

Table of Contents

1. Instrumentation and reagents:

Melting points were determined by MR-Vis$^+$ visual melting point range apparatus from LABINDIA instruments private limited. IR spectra were recorded on NICOLET iS5. HRMS data were obtained by Waters Xevo G-2XS QTOF spectrometer by ESI techniques. NMR spectra were recorded on Bruker 500 MHz FT-NMR spectrometers operating at ambient temperature. TMS was used as internal standard for ^{1}H NMR spectra. UV-Visible spectrum was recorded on Shimadzu UV-3600 spectrometer. Spectroscopic grade solvent was used for absorbance measurement. Cyclic voltammetry (CV) and differential pulse voltammetry (DPV) measurements were done using CH Instruments Electrochemical analyzer and electrodes were purchased from CH Instruments Inc. All measurements were performed in chloroform under flow of nitrogen and 0.1M tetrabutylammonium hexafluorophosphate ($TBAPF_6$) used as a supporting electrolyte. Glassy carbon as working electrode, platinum wire as counter electrode and Ag/AgCl in (1M) KCl as reference electrode were used. The redox potentials were referenced vs. sat. calomel electrode, SCE (0.48V for Fc^+ /Fc couple vs SCE). All cyclic voltammetry data were recorded at 100 mV/s scan rate.

Crystallographic data for **OAPo-T** and **OAPo-C** were collected on BRUKER APEX-II CCD microfocus diffractometer, Mo-K_α (λ = 0.71073 Å) radiation was used to collect X-ray reflections from their single crystals. Data reduction was performed using Bruker SAINT software.[S1] Intensities for absorption were corrected using and SADABS 2014/5,[S2] refined using SHELXL-2014/7[S3] with anisotropic displacement parameters for non-H atoms. Hydrogen atoms on O and N were experimentally located in difference electron density maps. All C−H atoms were fixed geometrically using HFIX command in SHELX-TL. A check of the final CIF file using PLATON[S4] did not show any missed symmetry.

Crystallographic data (including the structure factor) for structures **OAPo-T** and **OAPo-C** in this paper have been deposited in the Cambridge Crystallographic Data Centre as supplementary publication numbers CCDC1990315-1990316. Copies of the data can be obtained free of charge on application to CCDC, 12 Union Road, Cambridge CB2 1EZ, UK (Fax: +44(0)-1223-336033 or e-mail: deposit@ccdc.cam.ac.uk).

We have made use of a Ti-sapphire laser amplifier beam (Libra, M/s Coherent) for the Z-scan experiments with the following parameters: ~50 fs pulse duration, repetition rate of 1 kHz, beam diameters in the range of 2-2.5 mm. We utilized a 15-cm lens for focusing the beam onto the sample. We performed the experiment with corresponding Rayleigh range of 3.5-4.5 mm and used neutral density filters for input pulse energy attenuation. The fine powder-like samples were dissolved in DCM (~1.5 mM concentration) and they displayed a linear transmittance of 80-90% in the 800 nm and 1000 nm wavelength range. We have used a 1-mm glass cuvette for holding our solution sample. We utilized a lock-in to fetch together the transmittance data from photo-diode acquisition along with the stage position data received from a linear stage all together interfaced by a LabVIEW program. When any nonlinear optical material is scanned using a Gaussian laser pulse in the focal plane of a convex lens, the transmittance can be written in the following manner, both in open and closed aperture Z-scan methods,

$$Transmittance, T_{OA(2PA)} = \frac{1}{1 + \beta L_{eff}\left(\frac{I_{00}}{1 + \left(\frac{z}{z_0}\right)^2}\right)} \quad \ldots. (1)$$

$$Transmittance, T_{CA(2PA)} = \left(1 \pm \left(\frac{4\left(\frac{z}{z_0}\right)\Delta\Phi}{\left[9 + \left(\frac{z}{z_0}\right)^2\right]\left[1 + \left(\frac{z}{z_0}\right)^2\right]}\right)\right) \quad \ldots. (2)$$

Here sample effective length of the sample is estimated by $L_{eff}(cm^{-1}) = \frac{1 - e^{-\alpha L}}{\alpha}$ $(2PA)$, Rayleigh Range, defined by $Z_0(mm) = \frac{\pi\omega_0^2}{\lambda}$, Beam waist at focal point (z=0), $\omega_0(mm) = \frac{2.f.\lambda}{\pi.d}$, λ be wavelength and d be the waist at focal point. Now, the non-linear refractive index is to be evaluated from the relation $n_2(\frac{cm^2}{W}) = \frac{\Delta\Phi}{I_{0.}\, L_{eff.}\, k} = \frac{\Delta\Phi.\lambda}{I_{0.}\, L_{eff.}\, 2\pi}$. After all we can estimate both real, imaginary $\chi^{(3)}$ from the

following equations $Im\,|\chi^{(3)}|(m^2/V^2) = \frac{c\epsilon_0\lambda n_0^2\alpha_2(m/W)}{2\pi}$, $Re|\chi^{(3)}|(m^2/V^2) = 2c\epsilon_0 n_0^2 n_2\,(m^2/W)$ and finally $\chi^{(3)}$ total will emerge from the above both. Now we can use the relation $|\chi^{(3)}|(e.s.u) = \frac{(3\times10^4)^2|\chi^{(3)}|(m^2/V^2)}{4\pi}$ n for unit conversion of $\chi^{(3)}$. The errors in these measurements were estimated to be 5% arising from input laser fluctuations and errors in estimation of the beam waist at focus.

Commercially available solvents were distilled before use. Reagents were purchased from Sigma Aldrich, Merck and Spectrochem, India and used as received without further purification unless otherwise stated. Solvents for the reactions were dried according to literature methods.

2. Synthesis: Compound **5** was synthesized and characterized as per reported procedure.[S5]

2.1) 1,1'-(3,4-diethyl-1H,1'H-[2,2'-bipyrrole]-5,5'-diyl)bis(ethan-1-one)(6):

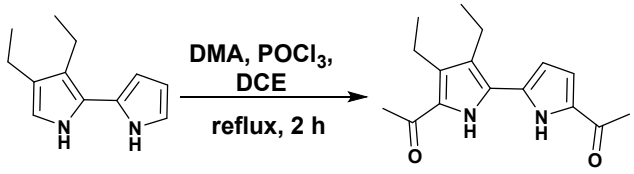

5 **6 (73%)**

The compound **5** (189 mg, 1mmol) in DCE (10 mL) was rapidly added to ice cooled stirred Vilsmeier acylating mixture prepared from $POCl_3$ (0.374 mL, 4 mmol) and N, N-dimethylacetamide (0.371 mL, 4 mmol) in DCE (10 mL) under nitrogen and then the reaction mixture was refluxed for 2 h. After cooling sodium acetate solution (5 mmol) was added at 0 °C and again refluxing continued for another 2 h. After cooling the reaction mixture to room temperature, organic layer was separated and water layer was extracted with chloroform for three times. Combined organic layer was passed through anhydrous Na_2SO_4 and evaporated to dryness to obtain a black solid. Crude reaction mixture was purified by silica gel column chromatography using EtOAc/ Hexane (3:7) and obtained as pale yellowish powder (200 mg).

Melting point: 205-207 ^oC; IR (KBr) (cm^{-1}): 3320, 2964, 1651, 1613, 1393; ^1H NMR (500 MHz, $CDCl_3$, δ in ppm): 11.63 (s, 1H), 11.13 (s, 1H), 7.04-7.02 (q, J = 2.3 Hz, 1H), 6.61-6.60 (q, J = 2.6 Hz, 1H), 2.84-2.80 (q, *J* = 7.6 Hz, 2H), 2.72-2.68 (q, *J* = 7.6 Hz, 2H), 2.65 (s, 3H), 2.57 (s, 3H), 1.27-1.21 (m, 6H) ; ^{13}C NMR (125 MHz, $CDCl_3$, δ in ppm): 188.5, 134.2, 132.2, 131.0, 128.9,

126.6, 119.4, 110.3, 27.6, 25.5, 18.6, 17.9, 16.3, 15.3; HRMS- (ESI+) m/z: calculated for $C_{16}H_{20}N_2O_2$ $[M+H]^+$: 273.1582; found: 273.1612.

2.2) Synthesis of 2,7,12,13-tetraethyl-9,10,19,20-tetramethylporphycene (OAPo-T) and 2,3,16,17-tetraethyl-9,10,19,20-tetramthylporphycene (OAPo-C).

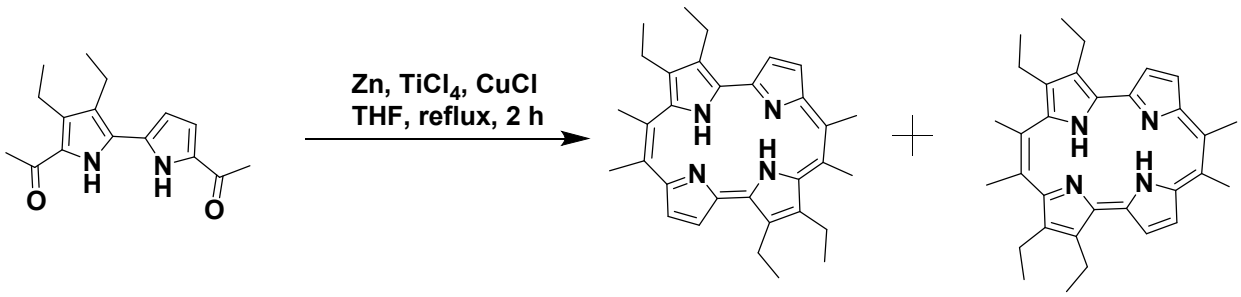

To a slurry of low-valent titanium reagent, generated by reduction of titanium tetrachloride (1.6 mL, 14.688 mmol) in dry THF (200 mL) with activated zinc (1.920 g, 29.3748mmol) and CuCl (291mg, 2.937 mmol) by refluxing for 2 h, a solution of bipyrrole dialdehyde (200 mg, 0.7344mmol) in dry THF (100 mL) was added dropwise slowly over 1 h under refluxing condition with vigorous stirring. The reaction mixture was heated under reflux for additional 2 h and then hydrolyzed by slow addition of 10% aqueous potassium carbonate (ca. 100 mL) to the ice cooled reaction mixture and filtered through celite to remove the excess metal, washed with ethyl acetate and organic layer was separated. Organic layer was evaporated to dryness under reduced pressure. Resulting crude reaction mixture was dissolved in chloroform (50 mL), washed with water, organic layer was passed through anhydrous sodium sulphate and evaporated to dryness under reduced pressure. The crude reaction mixture was purified by silica gel column chromatography using chloroform/hexane (15:85) as eluent to obtain mixture of both trans- and cis- isomers with 13% yield (23 mg). Further, both isomers (R_f = 0.41 for **OAPo-T** and R_f = 0.27 for **OAPo-C)** were purified and isolated through preparative thin layer chromatography by using DCM:hexane (25:75) solvent mixture as eluent with isolated yield of 8% (**OAPo-T,** 14.2 mg) and 5% **(OAPo-C,** 8.8 mg).

2,3,12,13-Tetraethyl-9,10,19,20-tetramethylporphycene, **OAPo-T** (purple solid): M.P. 310 °C; IR (KBr) (cm^{-1}): 2922, 2852, 1460, 1259, 1015; ^{1}H NMR (500 MHz, $CDCl_3$), δ (ppm): 9.25-9.24 (d, J = 4.5 Hz, 2H), 9.01-9.00 (d, J = 4.5 Hz, 2H), 5,67 (br, 2H), 4.02-3.97 (q, J = 7.6 Hz, 4H), 3.90 (s, 6H), 3.75-3.71 (m, 10H), 1.77-1.51 (m, 12H), ^{13}C NMR (125 MHz, $CDCl_3$), δ (ppm): 146.2, 143.0, 140.0, 139.4, 135.8, 132.0, 128.1, 125.1, 124.6, 124.0, 24.6, 23.9, 21.0, 20.6, 17.6, 16.9; HRMS (ESI+): m/z: calculated for $C_{32}H_{38}N_4$ [M+H]+ : 479.3174; found: 479.3175. UV-vis data, λ_{max} (in nm): 382, 613, 659, 691.

2,3,16,17-Tetraethyl-9,10,19,20-tetramethylporphycene, **OAPo-C** (purple solid): M.P. 323 °C; IR (KBr) (cm^{-1}): 2965, 2928, 1464, 1178, 1048 ; ^{1}H NMR (500 MHz, $CDCl_3$), δ (ppm): 9.21-9.20 (d, J = 4.4 Hz, 4H), 9.00-8.99 (d, J = 4.5 Hz, 4H), 6.92(br, 1H), 4.95 (br, 1H), 3.89-3.84 (m,

10H), 3.65 (s, 6H), 3.63-3.59 (q, J = 7.5 Hz, 4H) 1.70-1.65 (m, 12H); ^{13}C NMR (125 MHz, $CDCl_3$), δ (ppm): 145.0, 144.9, 139.0, 138.4, 135.7, 132.8, 127.9, 124.9, 124.5, 123.9, 23.9, 23.7, 21.6, 20.6, 17.5, 16.8; HRMS (ESI+): m/z: calculated for $C_{32}H_{38}N_4$ [M+H]+ : 479.3174; found: 479.3177. UV-vis data, λ_{max} (in nm): 384, 663.

3. ^{1}H and ^{13}C NMR spectra, and HRMS data:

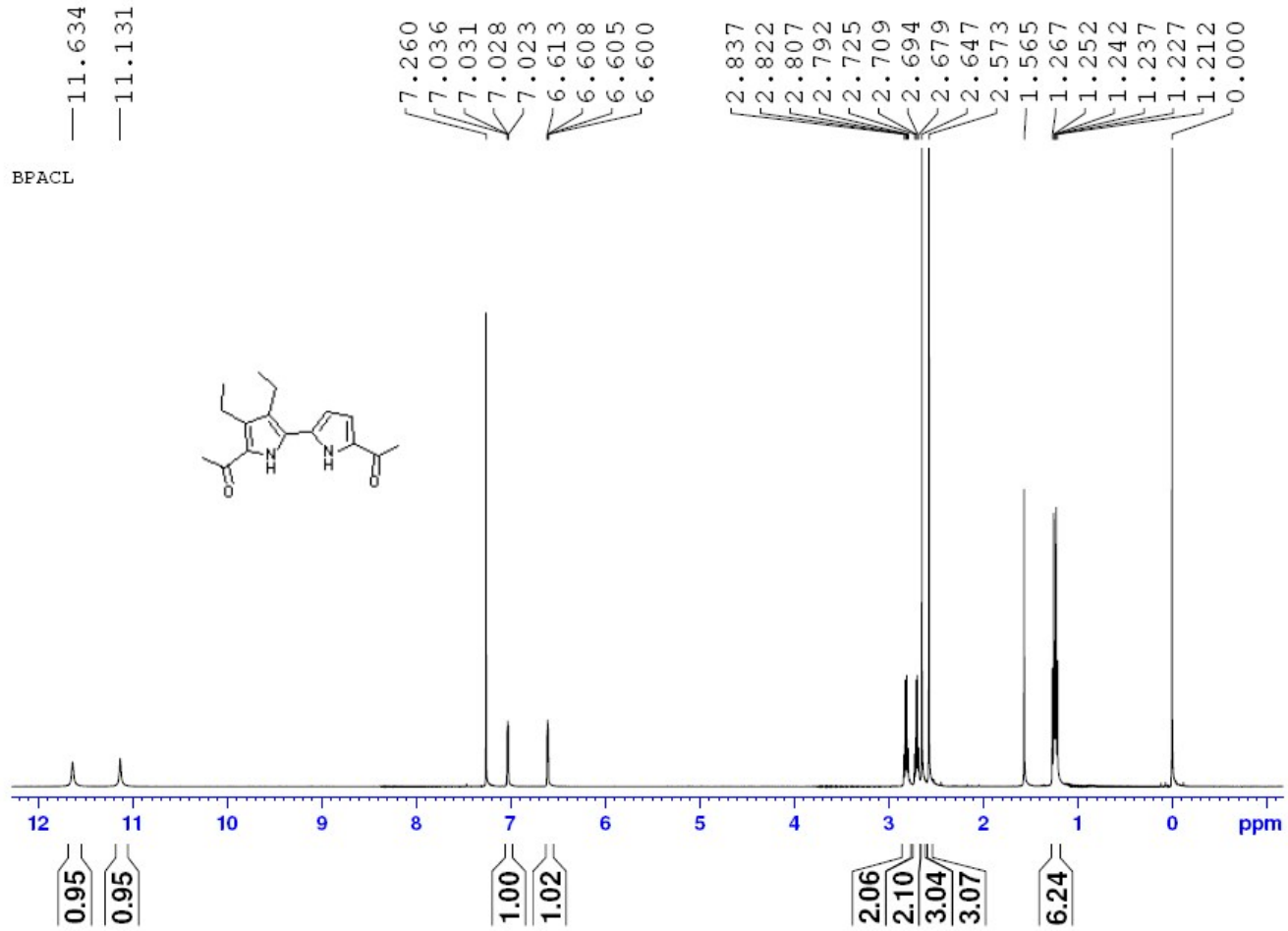

Figure S1: ^{1}H NMR spectrum of **6** in $CDCl_3$.

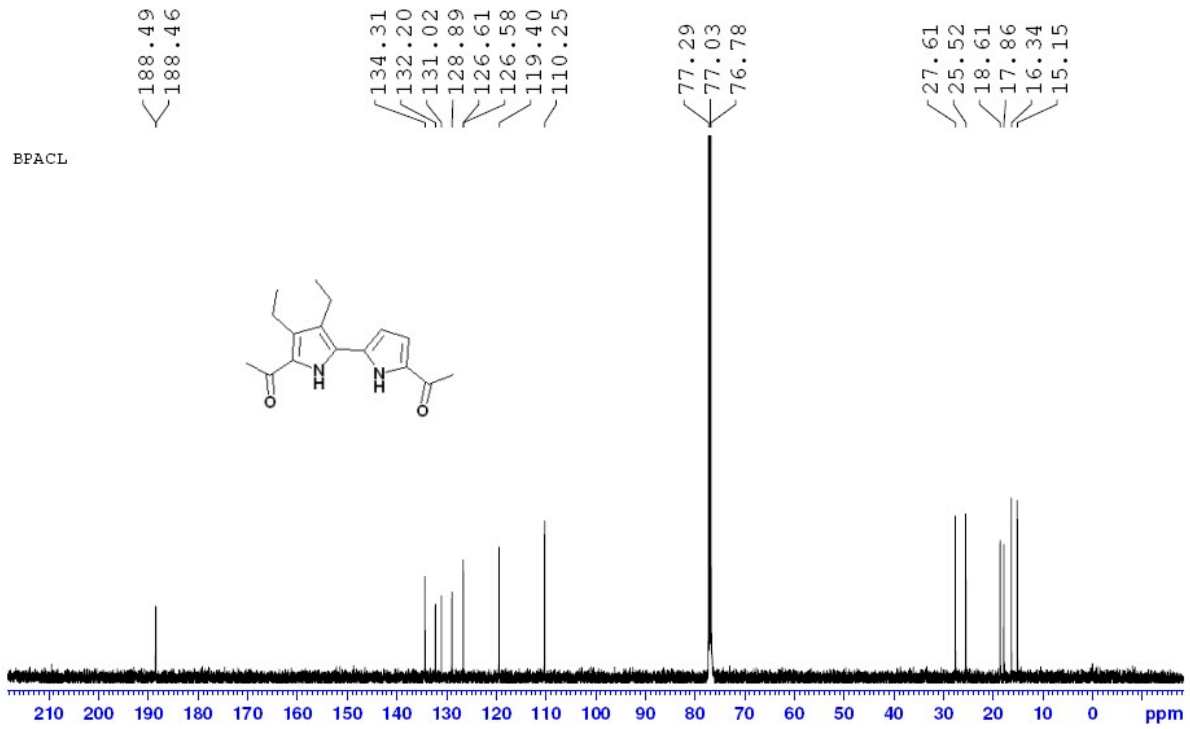

Figure S2: ^{13}C NMR spectrum of **6** in $CDCl_3$.

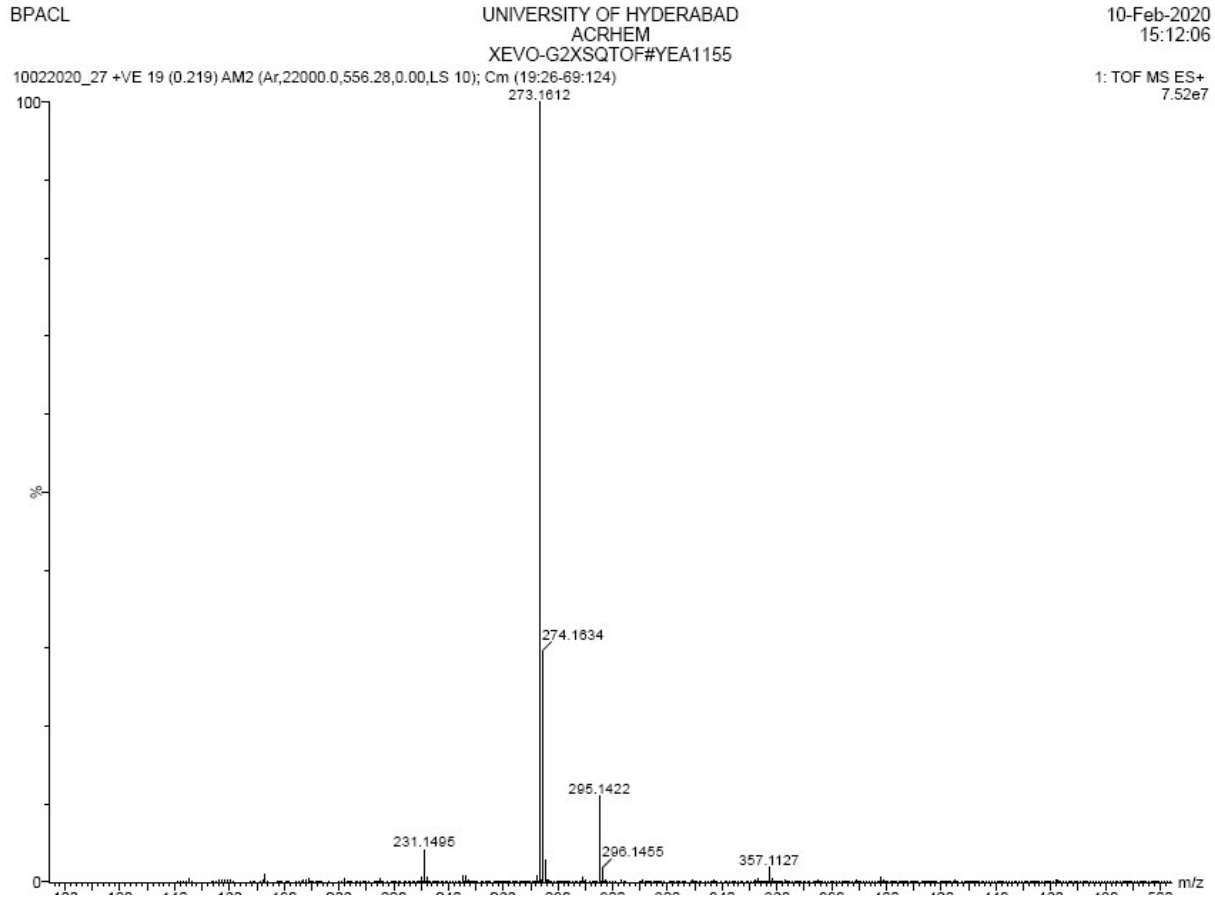

Figure S3: HRMS data of **6**.

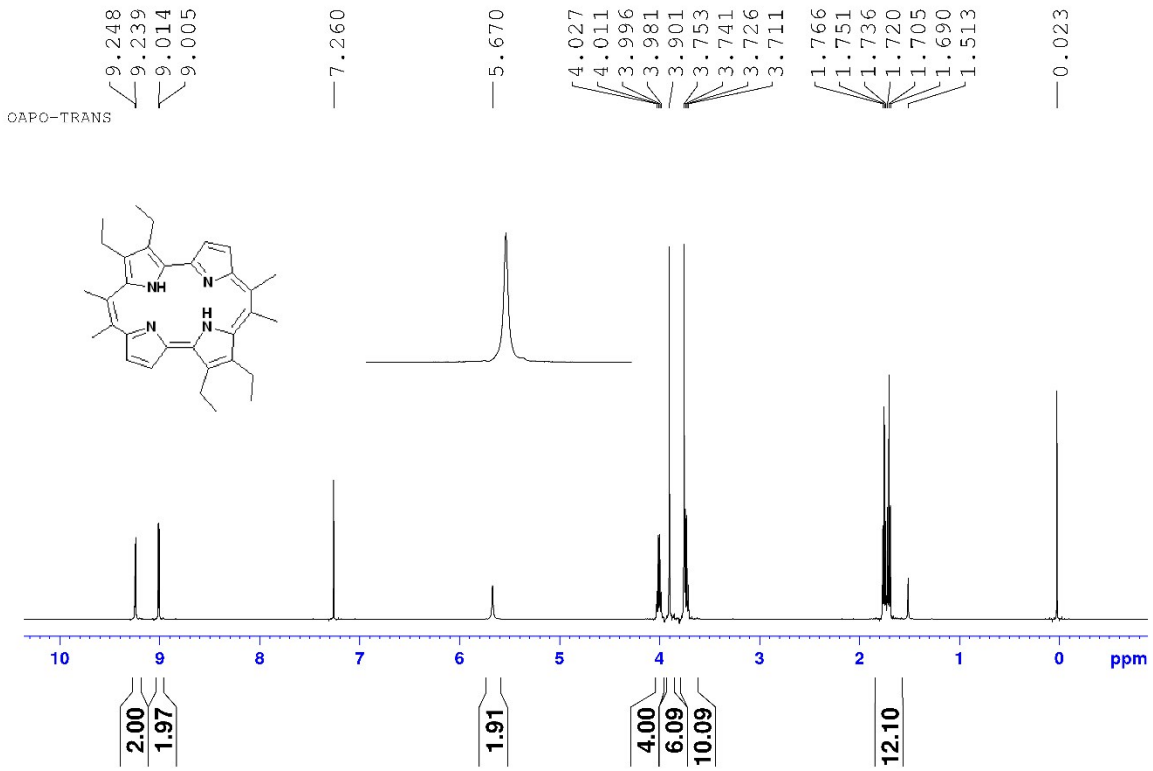

Figure S4: ^{1}H NMR spectrum of **OAPo-T** in $CDCl_3$.

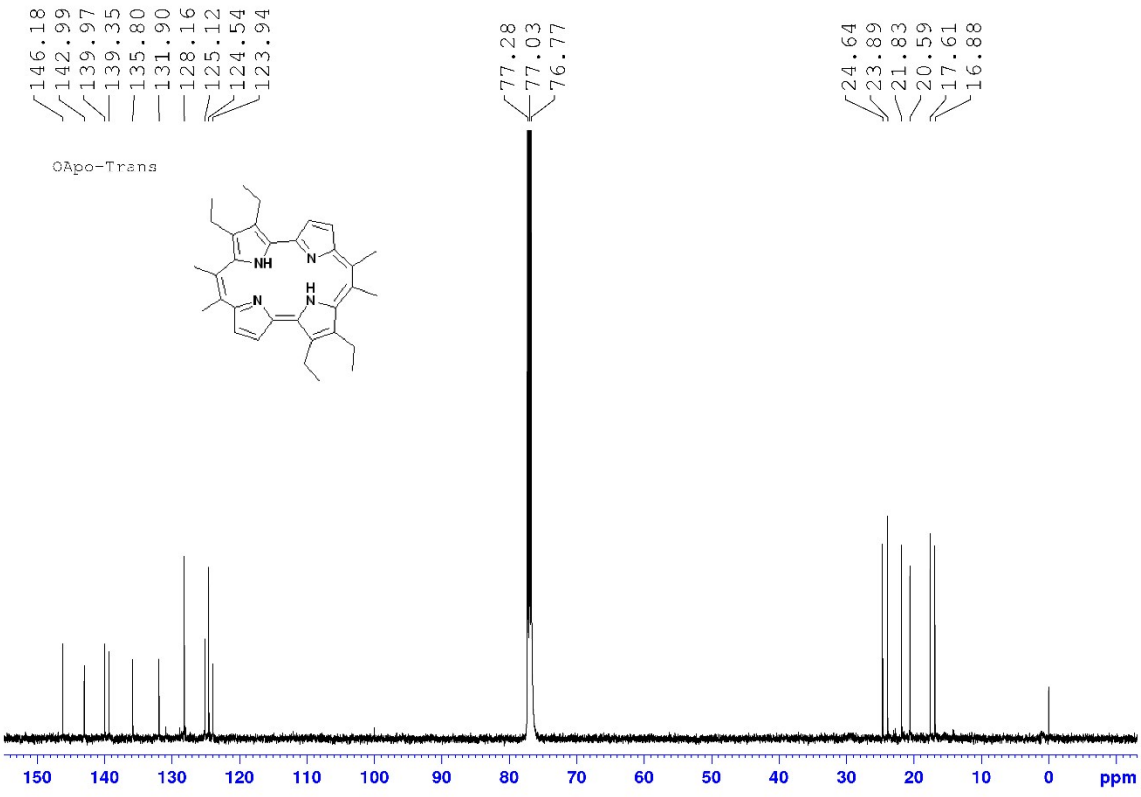

Figure S5: ^{13}C NMR spectrum of **OAPo-T** in $CDCl_3$.

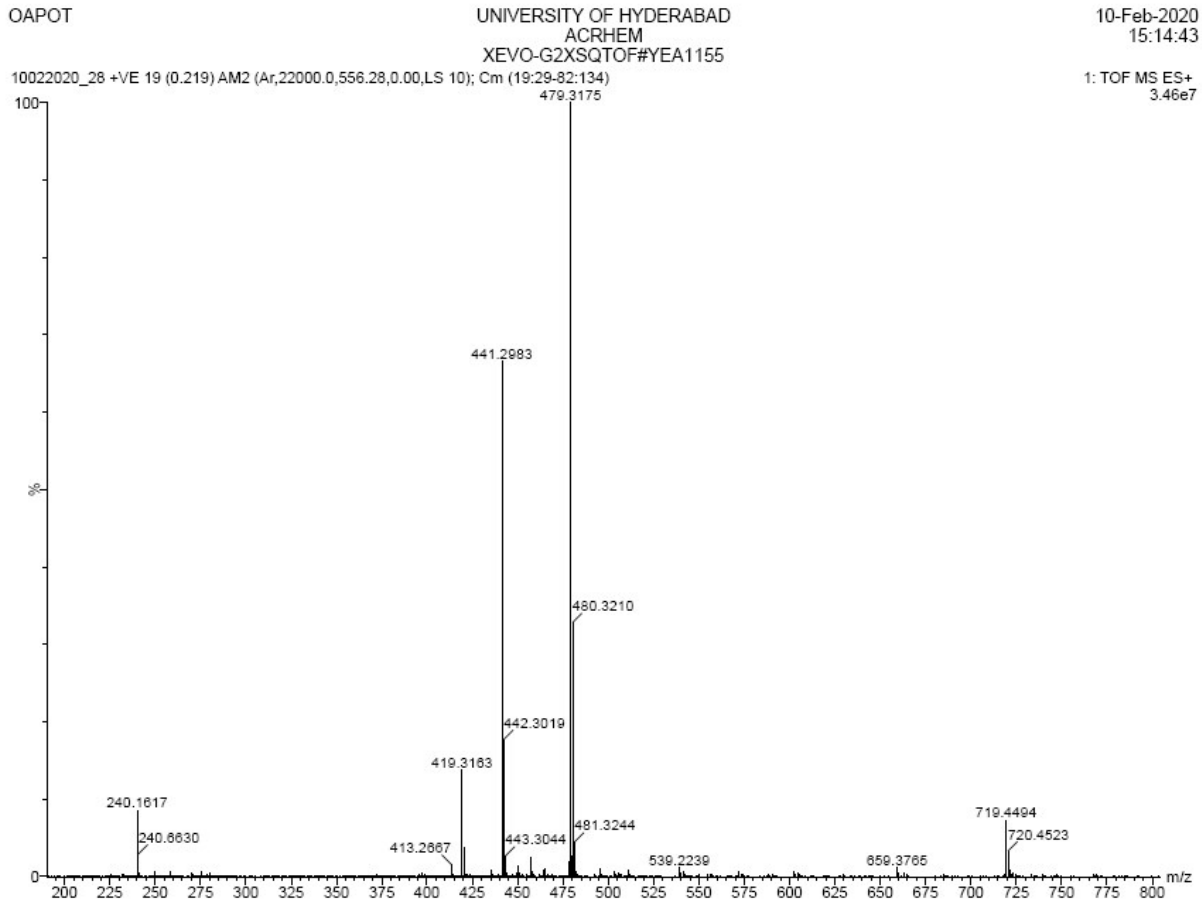

Figure S6: HRMS data of **OAPo-T**.

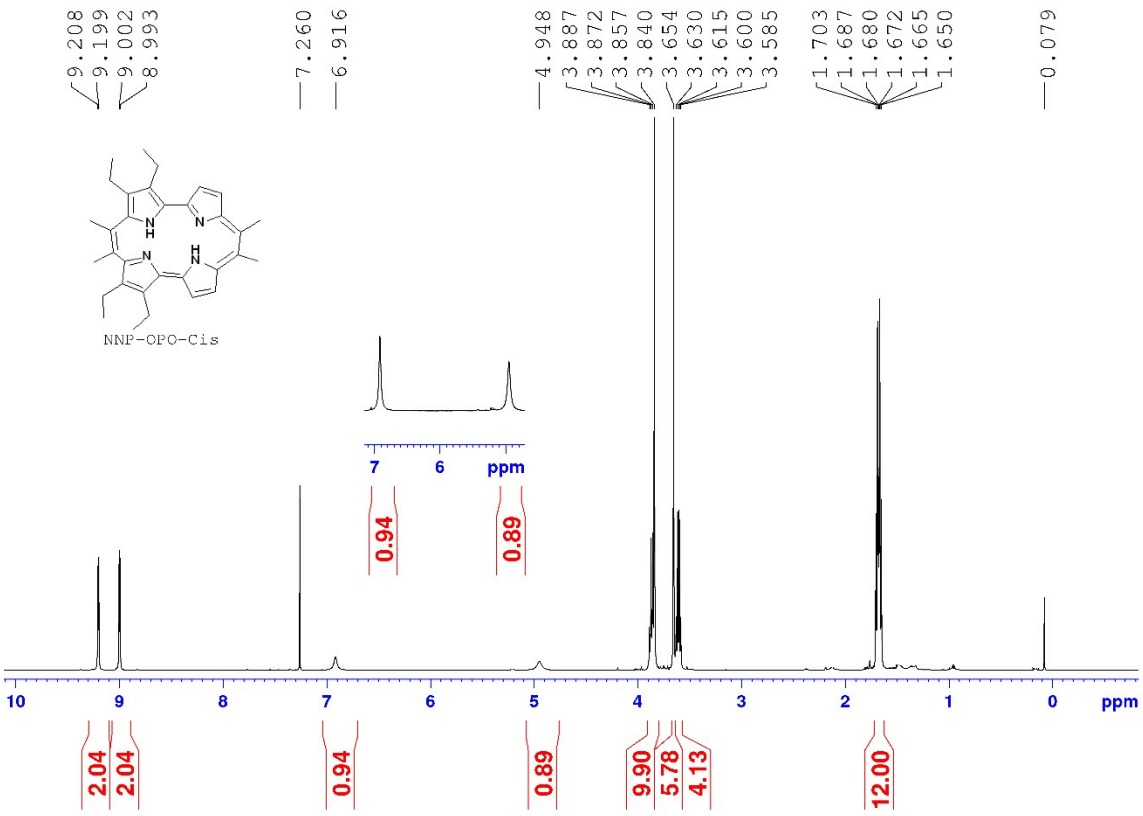

Figure S7: ^{1}H NMR spectrum of **OAPo-C** in $CDCl_3$.

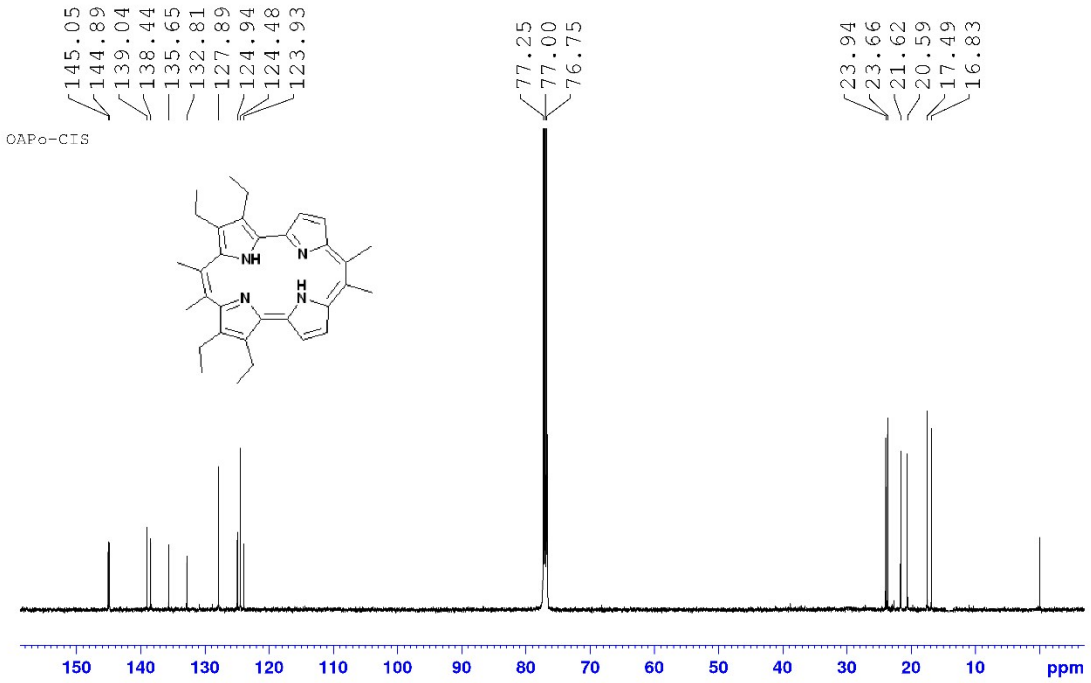

Figure S8: ^{13}C NMR spectrum of **OAPo-C** in $CDCl_3$.

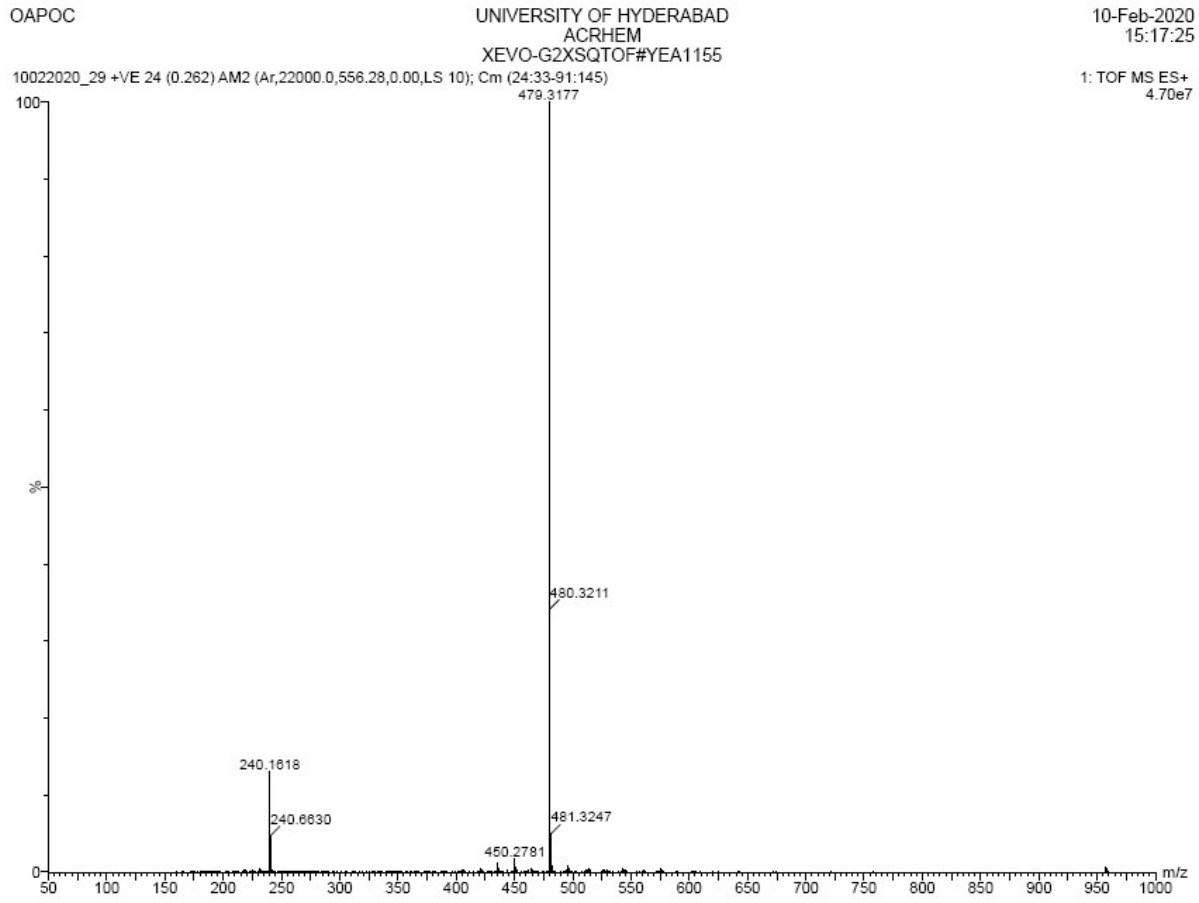

Figure S9: HRMS data of **OAPo-C**.

4. Preparative Thin Layer Chromatography.

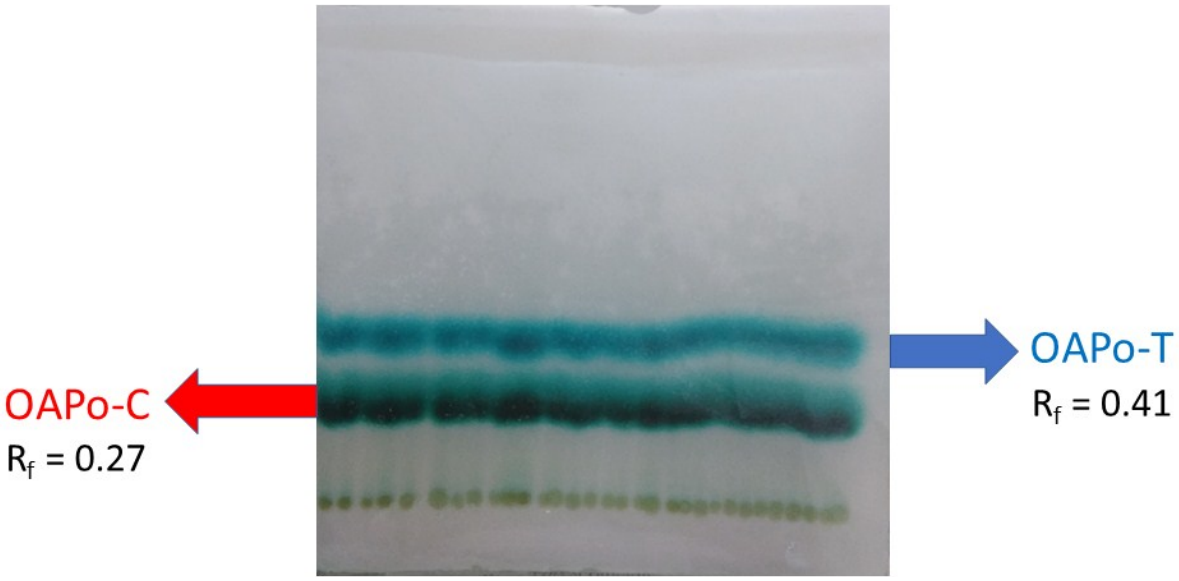

Figure S10 Preparative thin layer chromatography of **OAPo-C** and **OAPO-T**. Silica gel used as stationery phase and hexane:DCM (75:25) solvent mixture as eluent.

5. X-ray crystal structures:

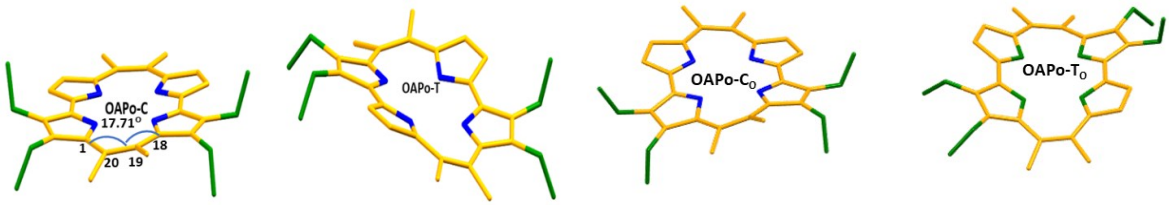

Figure S11 Crystal structure of **OAPo-C** and **OAPo-T** and optimized structure **OAPo-Co** and **OAPo-To** with ethyl groups orientation with torsion angle for **OAPo-C**. Color code: orange: C, blue: N, green: ethyl carbons.

Table S1: Skeletal deviations of the macrocycle atoms from the 24 atoms/4N mean plane for **OAPo-C** and **OAPo-T** and their optimized structure **OAPo-Co** and **OAPo-To**.

Label	OAPo-C (Crystal) Deviation from mean plane (Å)	OAPo-T (Crystal) Deviation from mean plane (Å)	OAPo-Co (Optimized) Deviation from mean plane (Å)	OAPo-To (Optimized) Deviation from mean plane (Å)
C1	**0.125**	**0.268**	**0.260**	**0.070**
C2	**0.166**	**0.196**	**0.225**	**0.398**
C3	**0.123**	**0.101**	**0.019**	**0.557**
C4	**0.057**	**0.109**	**0.034**	**0.174**
C5	**0.012**	**0.010**	**0.115**	**0.121**
C6	**0.066**	**0.267**	**0.196**	**0.336**
C7	**0.049**	**0.333**	**0.234**	**0.103**
C8	**0.172**	**0.075**	**0.157**	**0.254**
C9	**0.310**	**0.058**	**0.086**	**0.568**
C10	**0.350**	**0.304**	**0.162**	**0.424**
C11	**0.281**	**0.123**	**0.202**	**0.078**
C12	**0.257**	**0.147**	**0.302**	**0.384**
C13	**0.142**	**0.400**	**0.198**	**0.342**
C14	**0.107**	**0.277**	**0.052**	**0.195**
C15	**0.008**	**0.425**	**0.070**	**0.149**
C16	**0.141**	**0.917**	**0.327**	**0.562**
C17	**0.086**	**0.893**	**0.418**	**0.069**
C18	**0.047**	**0.367**	**0.184**	**0.266**
C19	**0.101**	**0.080**	**0.030**	**0.565**
C20	**0.118**	**0.285**	**0.374**	**0.048**
N1	**0.043**	**0.203**	**0.073**	**0.182**
N2	**0.120**	**0.127**	**0.091**	**0.214**
N3	**0.204**	**0.040**	**0.064**	**0.173**
N4	**0.077**	**0.107**	**0.013**	**0.191**

6: Theoretical studies

Quantum mechanical calculations were performed with Gaussian 09 program[S6] provided by CMSD facility of University of Hyderabad. All calculations were carried out by density functional theory (DFT) with Becke's three-parameter hybrid exchange functional and the Lee-Yang-Parr correlation functional (B3LYP) and the 6-31+G(d,p) basis set was used. The molecular orbitals were visualized using Gauss view 4.1 software. The theoretical excitation energies are obtained for the compounds by applying the TD-SCF method, which are visualized and tabulated by using

GaussSum 3.0 software. The nucleus independent chemical shift, NICS (0) values were obtained with gauge independent atomic orbital (GIAO) method based on the crystal structure geometries. [S7] HOMA (Harmonic Oscillator Model of Aromaticity) was calculated by using Ropt (C-C) = 1.388 Å and Ropt (C-N) = 1.334 Å[S8] based on the optimized geometries.

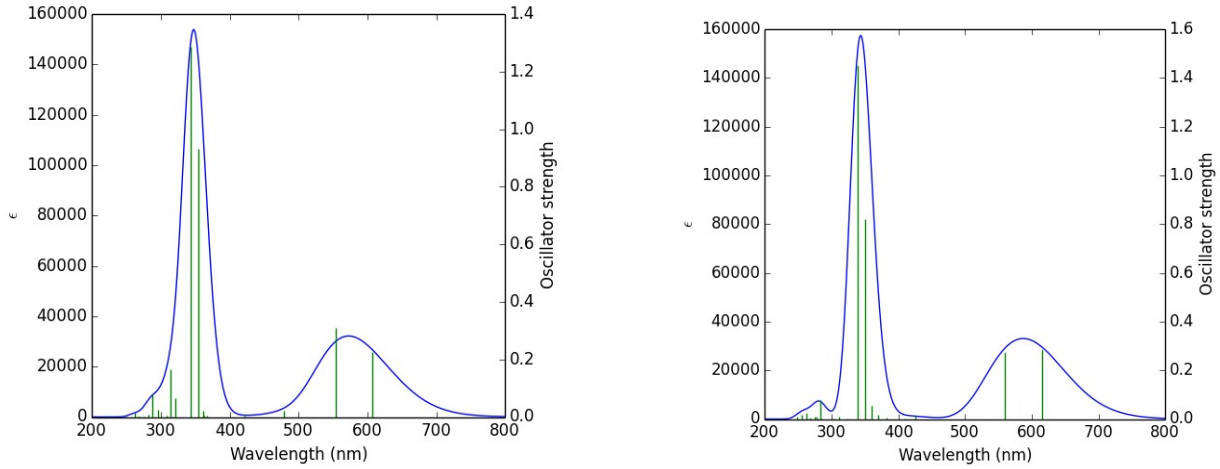

Figure S12: Theoretical absorption spectrum (by TD-DFT) of **OAPo-C** (left) and **OAPo-T**(right).

Table S2: Summary of theoretical excitation energies of **OAPo-C** in chloroform.

Sl. No.	Wavelength (nm)	Oscillator Strength	Major contributions
1	343	1.2864	H-1 → L+1 (73%), HOMO → LUMO (12%)
2	355	0.9309	H-1 → LUMO (12%), HOMO → L+1 (85%)
3	554	0.3095	H-1 → LUMO (74%), HOMO → LUMO (15%) HOMO → L+1 (9%)
4	608	0.2248	H-1→ LUMO (15%), HOMO → LUMO (72%), H-1 → L+1 (8%)

Table S3: Summary of theoretical excitation energies of **OAPo-T** in chloroform.

Sl. No.	Wavelength (nm)	Oscillator Strength	Major contributions
1	340	1.4521	H-5 → LUMO (14%), H-1 → L+1 (51%), HOMO → L+1 (17%), H-4 → LUMO (4%), H-1 → LUMO (4%), HOMO → LUMO (8%)
2	351	0.8194	H-1 → L+1 (27%), HOMO → L+1 (60%), H-1 → LUMO (8%)
3	559	0.2743	H-1 → LUMO (88%), HOMO → L+1 (12%)

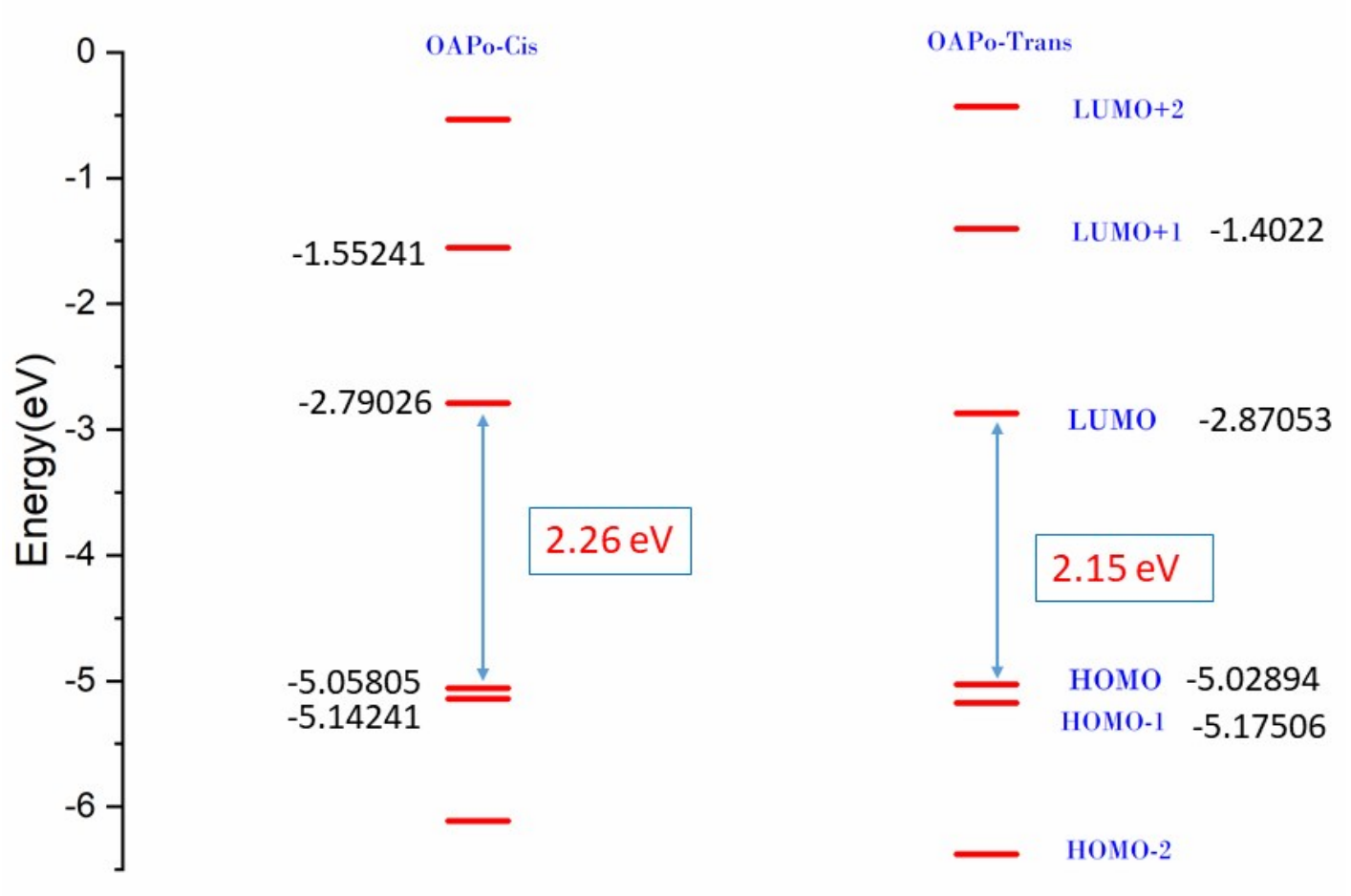

Figure S13: HOMO-LUMO energy diagram of **OAPo-C** and **OAPo-T**

Table S4: Summery of selected MO diagrams of DFT optimized structure of OAPo-C.

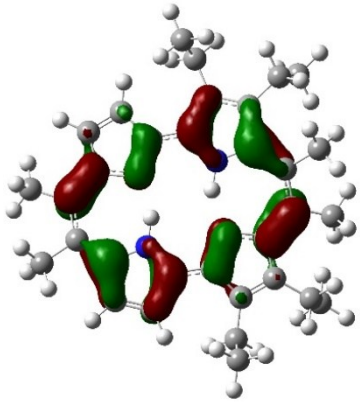	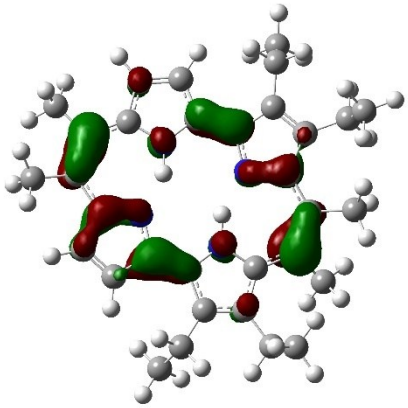
HOMO	HOMO-1

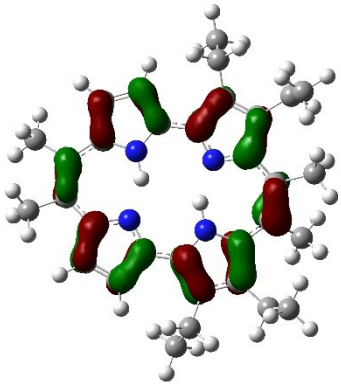	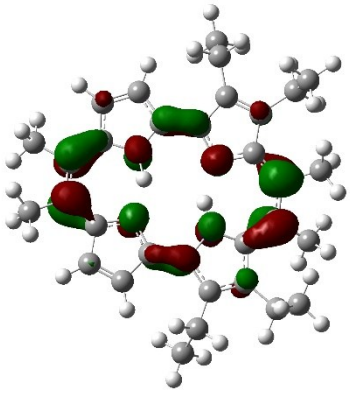
LUMO	LUMO+1

Table S5: Summery of selected MO diagrams of DFT optimized structure of OAPo-T.

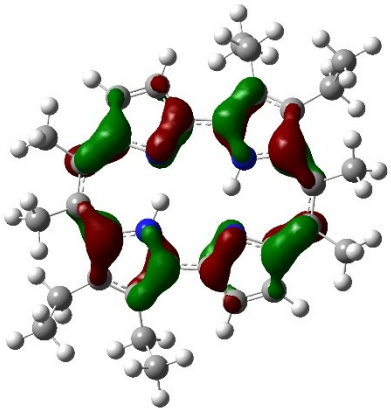	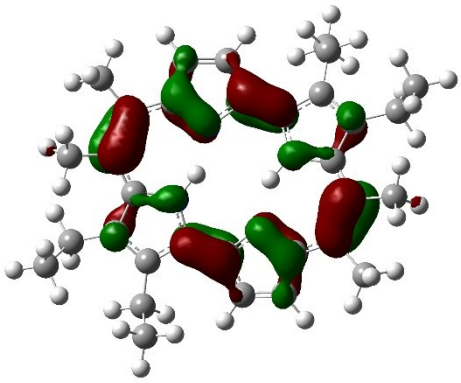
HOMO	HOMO-1
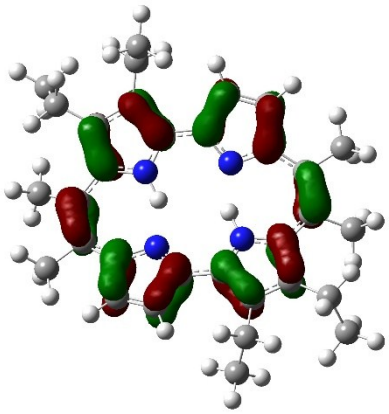	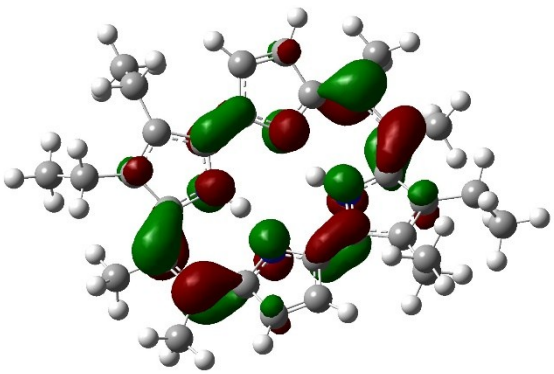
LUMO	LUMO+1

Table S6. Summary of calculated NICS (0) and HOMA values.

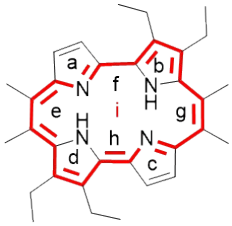

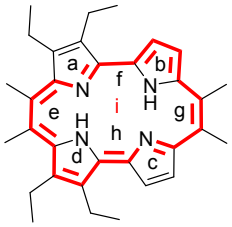

ICS value for **OAPo-T**	Labels	NICS value for **OAPo-C**
-5.195	a	-3.466
-10.802	b	-12.019
-5.195	c	-4.894
-10.802	d	-10.161
-16.019	e	-16.17
-23.918	f	-24.87
-16.019	g	-16.17
-23.987	h	-25.06
-11.835	i	-11.93

Macrocycle	HOMA
OAPo-C	0.562
OAPo-T	0.466

7. Electrochemical study.

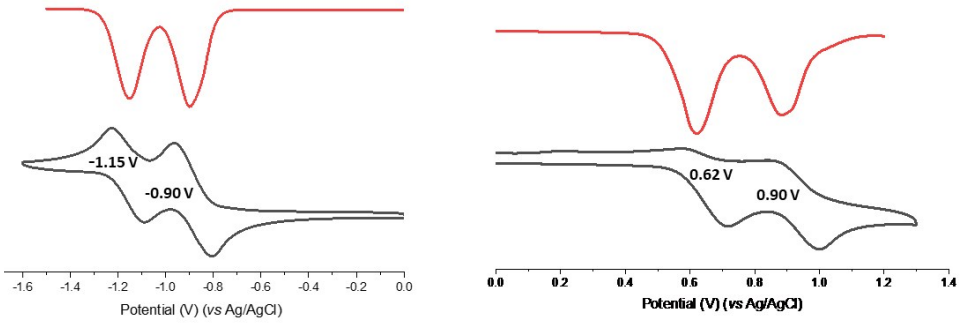

Fig. S14 Cyclic voltammogram (black line) and differential pulse voltammogram (red line) of **OAPo-T** vs Ag/AgCl in DCM.

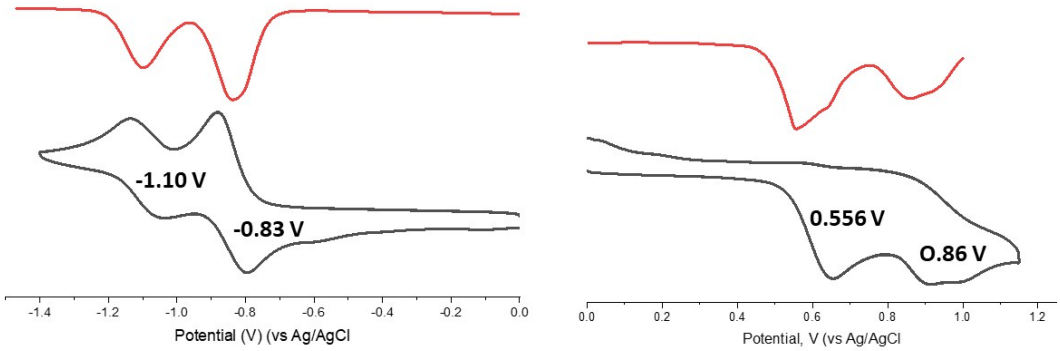

Fig. S15 Cyclic voltammogram (black line) and differential pulse voltammogram (red line) of **OAPo-C** vs Ag/AgCl in DCM.

8. Tautomeric forms of OAPo-C and OAPo-T:

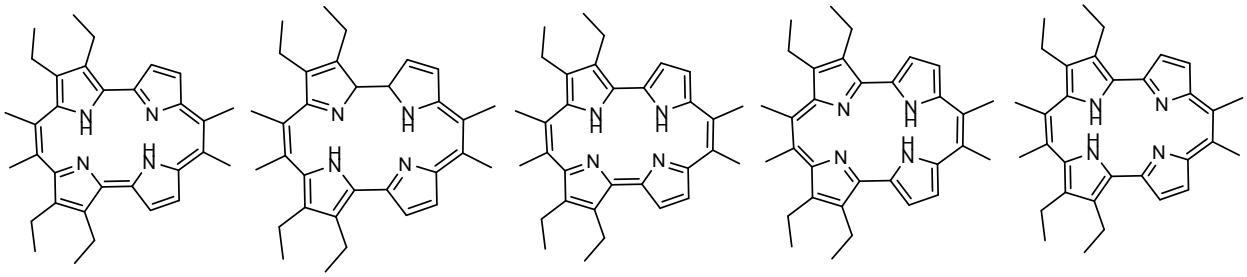

Fig. S16 Different tautomeric forms of **OAPo-C**.

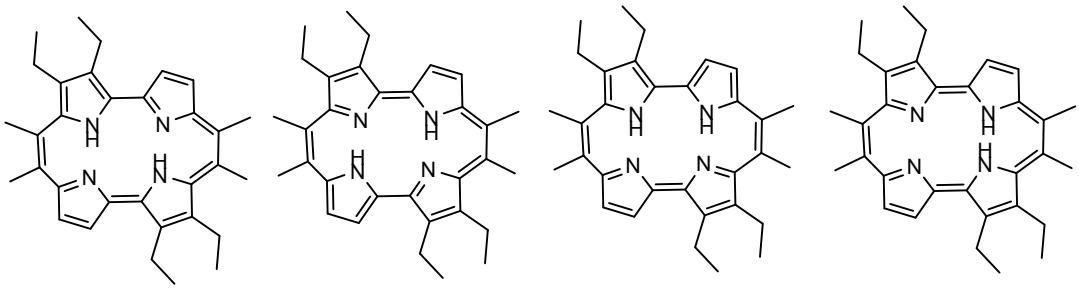

Fig. S17 Different tautomeric forms of **OAPo-T**.

9. NLO properties of OAPo-C and OAPo-T.

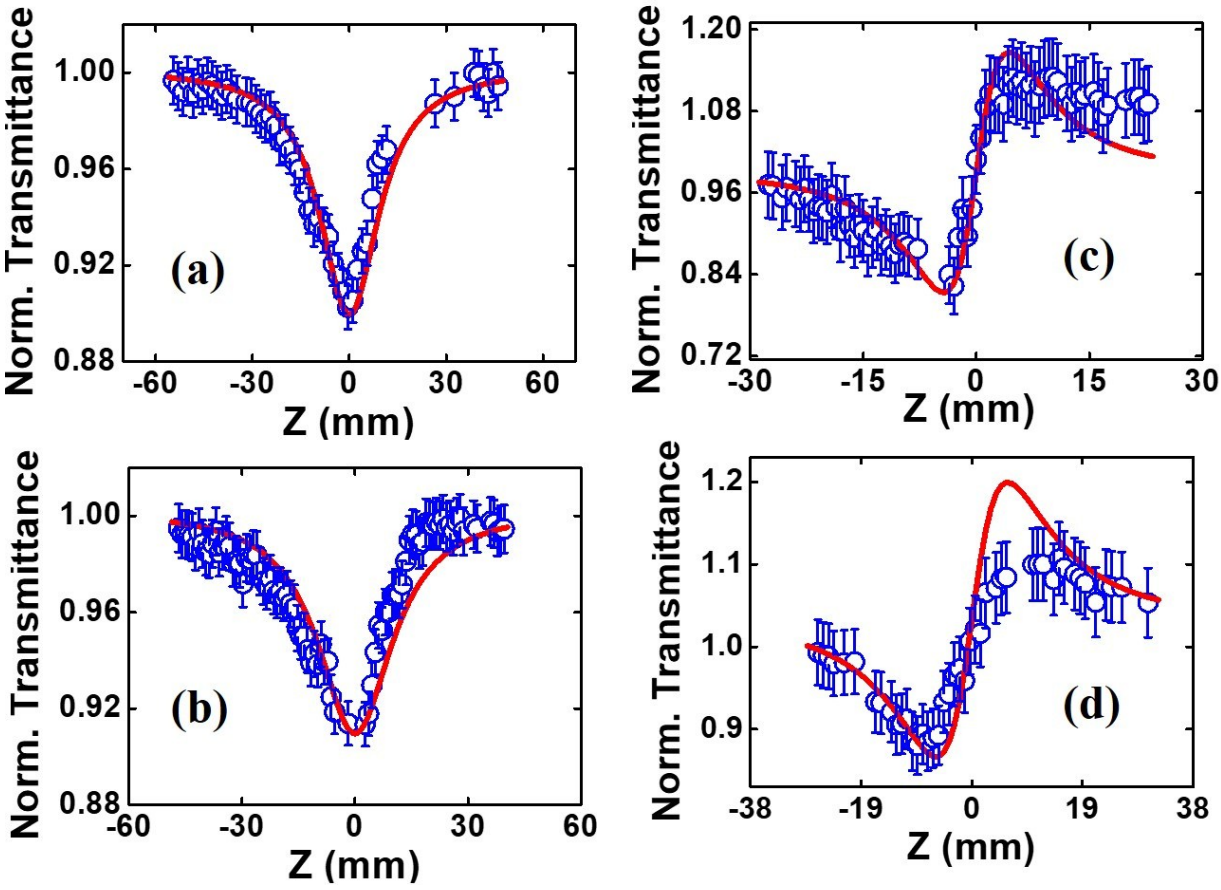

Fig. S18 Experimental and theoretically fitted Z-scan data for sample **OAPo-T** & **OAPo-C** in OA mode (a & b) and CA mode (c & d) at 1000 nm. Open symbols are experimental data while the solid lines are theoretical fits to the data.

Table S7: NLO properties of OAPo-C and OAPo-T*

λ (nm)	**$\beta\times10^{-11}$ (cm W^{-1})**	**σ_{2PA}(GM)**	**Im ($\chi^{(3)}$) $\times10^{-15}$ (e.s.u.)**	**$n_2\times10^{-15}$ (cm^2 W^{-1})**	**Re($\chi^{(3)}$) $\times10^{-15}$ (e.s.u.)**	**Total ($\chi^{(3)}$) $\times 10^{-15}$ (e.s.u.)**
OAPo-C						
800	0.4	145	1.97	0.259 (-ve)	19.9	20
1000	0.069	20	0.43	0.08 (+ve)	6.18	6.2
OAPo-T						
800	0.44	159.1	2.16	0.34 (+ve)	26.7	26.8
1000	0.079	21.7	0.49	0.1 (+ve)	7.72	7.74

*Error margin: ± 5%.

10. Coordinates of optimised geometry

Table S8: Coordinates of optimised geometry of OAPo-T

Atomic label	Symbol	X	Y	Z	Atomic label	Symbol	X	Y	Z
1	N	-1.99172	-0.06314	-0.12156	38	H	-2.97075	-4.67837	-1.83235
2	H	-1.07136	-0.54461	-0.27412	39	C	-0.00397	-4.14165	0.236794
3	N	0.127155	1.861496	-0.06165	40	H	-0.2969	-5.16586	0.413575
4	N	2.008375	0.035691	-0.20572	41	C	6.569851	-0.36827	-1.11405
5	N	-0.10937	-1.89343	-0.21307	42	H	6.438724	-1.42585	-1.36327
6	C	-1.13475	2.163475	0.3439	43	H	7.635446	-0.19312	-0.92847
7	C	2.229127	-1.282	0.068425	44	H	6.283241	0.206569	-2.00034
8	C	-2.19743	1.224878	0.277683	45	C	1.254554	-3.63864	0.402339
9	C	3.257132	2.146895	-0.52223	46	H	2.126142	-4.18984	0.717799
10	C	-3.60473	1.368776	0.538836	47	C	-4.59879	3.647996	-0.07943
11	C	0.05854	4.052076	0.620944	48	H	-3.67489	4.001168	-0.54583
12	H	0.365154	5.052452	0.887639	49	H	-5.12406	4.514875	0.337336
13	C	3.649808	-1.45077	0.215269	50	H	-5.22325	3.221152	-0.87039
14	C	3.180867	0.739123	-0.28201	51	C	-5.6577	-0.16344	0.567147
15	C	-1.19414	3.537478	0.791457	52	H	-5.78956	-1.23462	0.730949
16	H	-2.0483	4.056659	1.196196	53	H	-5.90855	0.304209	1.527451
17	C	4.24535	-0.2154	-0.01929	54	C	2.735415	4.57813	-0.45298
18	C	0.891533	2.986394	0.07991	55	H	3.668469	4.777949	0.082999
19	C	-3.1625	-0.77086	-0.16148	56	H	1.99572	5.294526	-0.10779
20	C	-2.25633	-3.14953	-0.46529	57	H	2.917614	4.810472	-1.51005
21	C	-0.86284	-3.03164	-0.15167	58	C	-4.61846	-2.59747	-1.05088
22	C	1.17126	-2.22673	0.101172	59	H	-4.49529	-3.21471	-1.94536
23	C	-3.25671	-2.15001	-0.53283	60	H	-5.23226	-1.75126	-1.34421
24	C	2.267315	3.134639	-0.28919	61	H	-5.18537	-3.20072	-0.32993
25	C	-4.2074	0.142383	0.266701	62	C	-6.67622	0.329457	-0.48019
26	C	-4.31591	2.605639	1.02275	63	H	-6.64756	1.418467	-0.57678
27	H	-3.74426	3.073686	1.831319	64	H	-7.69342	0.044704	-0.18886
28	H	-5.26945	2.310667	1.473481	65	H	-6.48056	-0.08873	-1.47301
29	C	5.732866	0.017906	0.123422	66	C	4.341093	-2.99632	2.126122
30	H	6.089373	-0.57674	0.972656	67	H	4.80606	-2.17978	2.688609
31	H	5.936116	1.055251	0.396919	68	H	4.882965	-3.91987	2.359408
32	C	4.380043	-2.70867	0.611113	69	H	3.314504	-3.10167	2.489406
33	H	5.425293	-2.63069	0.298329	70	H	1.083044	0.528577	-0.26701
34	H	3.977429	-3.56461	0.060203	71	C	4.588318	2.649417	-1.06687
35	C	-2.72785	-4.56895	-0.76763	72	H	4.420436	3.377827	-1.86457
36	H	-3.62765	-4.83944	-0.20645	73	H	5.169534	1.844699	-1.5058
37	H	-1.96597	-5.31248	-0.55193	74	H	5.208967	3.148884	-0.31149

Table S9: Coordinates of optimised geometry of OAPo-C

Atomic label	Symbol	X	Y	Z	Atomic label	Symbol	X	Y	Z
1	N	-0.76876	-1.35042	-0.10199	38	C	-4.03763	-3.08982	0.270542
2	N	-2.18439	1.144564	0.18717	39	H	-4.50655	-2.46476	1.034884
3	N	1.503974	0.005239	-0.15419	40	H	-4.02645	-4.09847	0.695941
4	N	0.022208	2.502115	-0.07613	41	C	1.181262	-4.38969	-1.21954
5	C	2.467184	-0.96596	-0.03055	42	H	1.175142	-5.25167	-0.54172
6	C	-2.81435	-0.05985	0.228828	43	H	2.125505	-4.41546	-1.76531
7	C	1.386069	2.43143	-0.14672	44	H	0.396132	-4.5386	-1.96091
8	C	-0.35284	-2.63804	-0.33511	45	C	3.392319	-3.30423	0.010515
9	C	2.110943	1.208011	-0.08765	46	H	4.034192	-3.40002	-0.87483
10	C	-2.11832	-1.2865	0.086476	47	H	3.055099	-4.30602	0.275986
11	C	0.996204	-3.03401	-0.53581	48	H	4.011943	-2.96644	0.836388
12	C	-1.54552	-3.47341	-0.24315	49	C	5.565496	-1.10246	1.801115
13	C	-0.41517	3.800168	-0.16714	50	H	5.511697	-0.16968	2.371896
14	C	3.548318	1.048595	0.082752	51	H	6.587381	-1.49094	1.878274
15	C	3.784892	-0.30622	0.137081	52	H	4.894439	-1.81558	2.29129
16	C	2.210685	-2.35758	-0.19175	53	C	-4.18137	4.372221	0.535953
17	C	-3.13015	2.119596	0.32604	54	H	-3.94627	5.275049	1.103194
18	C	-2.6175	-2.63796	0.03989	55	H	-4.91229	3.821239	1.123862
19	C	-1.75914	4.266007	-0.03947	56	H	-4.67491	4.691635	-0.39178
20	C	-2.92979	3.538583	0.2663	57	C	5.143217	2.606491	-1.16956
21	C	1.85837	3.770612	-0.29834	58	H	5.622912	1.7807	-1.70548
22	H	2.885379	4.077203	-0.40491	59	H	5.887171	3.399948	-1.03402
23	C	-4.23679	0.137572	0.397199	60	H	4.346674	2.991238	-1.81414
24	H	-5.00385	-0.61825	0.444289	61	C	-1.91554	5.772629	-0.2282
25	C	5.181116	-0.85944	0.326098	62	H	-2.83069	6.01347	-0.77301
26	H	5.890627	-0.13671	-0.08995	63	H	-1.09287	6.193443	-0.80342
27	H	5.337678	-1.76932	-0.25438	64	H	-1.9563	6.308289	0.72955
28	C	-4.43276	1.486969	0.469092	65	C	-1.22691	-5.61187	1.108647
29	H	-5.38958	1.975428	0.574833	66	H	-0.18391	-5.37753	1.34365
30	C	-1.66168	-4.98001	-0.22999	67	H	-1.33276	-6.70208	1.075455
31	H	-1.10257	-5.44051	-1.04479	68	H	-1.84	-5.23485	1.933954
32	H	-2.70639	-5.24646	-0.41512	69	C	-4.90336	-3.10278	-1.00552
33	C	4.594239	2.129941	0.19123	70	H	-4.95926	-2.10966	-1.46136
34	H	5.431204	1.7627	0.794074	71	H	-5.92318	-3.43403	-0.77933
35	H	4.193114	2.981308	0.749129	72	H	-4.48305	-3.7843	-1.75267
36	C	0.762101	4.604484	-0.32447	73	H	-0.06409	-0.57241	-0.13648
37	H	0.796399	5.678184	-0.42239	74	H	-0.68055	1.7224	0.036402

11. References:

S1 SAINT, version 6.45 /8/6/03 and version 8.34A, Bruker AXS, 2003**,** 2014.

S2 G. M. Sheldrick, SADABS and SADABS 2014/5, *Program for Empirical Absorption Correction of Area Detector Data,* University of Göttingen, Germany, 1997**,** 2014.

S3 (a) SHELXL -Version 2014/7; *Program for the Solution and Refinement of Crystal Structures,* University of Göttingen, Germany, 1993-2014; (b) G. M. Sheldrick, *Acta Cryst.* 2008, **A64**, 112.

S4 (a) A. L. Spek, *PLATON*, *A Multipurpose Crystallographic Tool*, Utrecht University, Utrecht, The Netherlands, 2002. (b) A. L. Spek, *J. Appl. Cryst.,* 2003, **36**, 7.

S5 N. N. Pati, B. S. Kumar, B. Chandra and P. K. Panda, *Eur. J. Org. Chem.,* 2017, 741.

S6 M. J. Frisch, G. W. Trucks, H. B. Schlegel, G. E. Scuseria, M. A. Robb, J. R. Cheeseman, G. Scalmani, V. Barone, B. Mennucci, G. A. Petersson, H. Nakatsuji, M. Caricato, X. Li, H. P. Hratchian, A. F. Izmaylov, J. Bloino, G. Zheng, J. L. Sonnenberg, M. Hada, M. Ehara, K. Toyota, R. Fukuda, J. Hasegawa, M. Ishida, T. Nakajima, Y. Honda, O. Kitao, H. Nakai, T. Vreven, J. A. Montgomery, Jr., J. E. Peralta, F. Ogliaro, M. Bearpark, J. J. Heyd, E. Brothers, K. N. Kudin, V. N. Staroverov, R. Kobayashi, J. Normand, K. Raghavachari, A. Rendell, J. C. Burant, S. S. Iyengar, J. Tomasi, M. Cossi, N. Rega, J. M. Millam, M. Klene, J. E. Knox, J. B. Cross, V. Bakken, C. Adamo, J. Jaramillo, R. Gomperts, R. E. Stratmann, O. Yazyev, A. J. Austin, R. Cammi, C. Pomelli, J. W. Ochterski, R. L. Martin, K. Morokuma, V. G. Zakrzewski, G. A. Voth, P. Salvador, J. J. Dannenberg, S. Dapprich, A. D. Daniels, Ö. Farkas, J. B. Foresman, J. V. Ortiz, J. Cioslowski, and D. J. Fox, *Gaussian 09* (Gaussian, Inc., Wallingford CT, 2009).

S7 (a) P. von R. Schleyer, C. Maerker, A. Dransfeld, H. Jiao and N. J. R. van Eikema Hommes, *J. Am. Chem. Soc*., 1996, **118**, 6317-6318; (b) Z. Chen, C. S. Wannere, C. Corminboeuf, R. Puchta and P. von R. Schleyer, *Chem. Rev.*, 2005, **105**, 3842-3888.

S8 (a) T. M. Krygowski and M. Cryanski, *Tetrahedron,* 1996, **52**, 1713-1722; (b) T. M. Krygowski and M. Cryanski, *Tetrahedron,* 1996, **52**, 10255-10264; (c) T. M. Krygowski and M. Cryanski, *Chem. Rev.,* 2001, **101,** 1385-1419.